nature chemistry

ARTICLES

PUBLISHED ONLINE: 7 FEBRUARY 2010 | DOI: 10.1038/NCHEM.547

Anisotropic oxygen diffusion at low temperature in perovskite-structure iron oxides

Satoru Inoue[1], Masanori Kawai[1], Noriya Ichikawa[1], Hiroshi Kageyama[2], Werner Paulus[3] and Yuichi Shimakawa[1]*

Oxygen-ion conduction in transition-metal oxides is exploited in, for example, electrolytes in solid-oxide fuel cells and oxygen-separation membranes, which currently work at high temperatures. Conduction at low temperature is a key to developing further utilization, and an understanding of the structures that enable conduction is also important to gain insight into oxygen-diffusion pathways. Here we report the structural changes observed when single-crystalline, epitaxial $CaFeO_{2.5}$ thin films were changed into $CaFeO_2$ by low-temperature reductions with CaH_2. During the reduction process from the brownmillerite $CaFeO_{2.5}$ into the infinite-layer structure of $CaFeO_2$, some of the oxygen atoms are released from and others are rearranged within the perovskite-structure framework. We evaluated these changes and the reaction time they required, and found two oxygen diffusion pathways and the related kinetics at low temperature. The results demonstrate that oxygen diffusion in the brownmillerite is highly anisotropic, significantly higher along the lateral direction of the tetrahedral and octahedral layers.

The iron oxides $SrFeO_2$ and $CaFeO_2$ crystallize in the infinite-layer structure that consists of FeO_2 planes with corner-sharing, square-planar oxygen coordination of divalent Fe ions[1–4]. The square-planar oxygen coordination of Fe^{2+} in this structure is uncommon because Fe ions in oxides are usually coordinated tetrahedrally or octahedrally by oxygen ions. The lack of apical oxygen atoms makes the crystal structure of $SrFeO_2$ highly anisotropic and causes this material to show two-dimensional magnetism with an unusually high antiferromagnetic Néel temperature[1]. The compound is obtained by reducing $SrFeO_{2.875}$ or $SrFeO_{2.5}$ at 280 °C with CaH_2 (refs 5–7). Although the brownmillerite structure $SrFeO_{2.5}$ with Fe^{3+} had been assumed to represent the lower limit of oxygen non-stoichiometry in the $SrFeO_{3-\delta}$ perovskites[8–11], low-temperature reduction with CaH_2 enabled us to go below that presumed limit. As for $SrFeO_{2.5}$, the brownmillerite $CaFeO_{2.5}$ can be reduced to $CaFeO_2$ with an infinite-layer structure by the same method[2]. The coordination of the high-spin Fe^{2+} in $CaFeO_2$ is slightly distorted from the perfect square-planar coordination of $SrFeO_2$, a distortion that occurs because Ca^{2+} is smaller than Sr^{2+} (ref. 4).

During the reduction of the fully oxygenated perovskite $AFeO_3$ (A = Ca or Sr) to the infinite-layer structure $AFeO_2$, oxygen ions are removed from the perovskite-structure framework and several distinct phases with ordered arrangements of oxygen vacancies appear. Such vacancies produce both oxygen-ion conduction and electronic conduction, and the former could be exploited in electrolytes in solid-oxide fuel cells and in oxygen-separation membranes. The oxygen-ion conduction in solids is ascribed generally to hopping by way of vacant atomic sites[12,13], and so an understanding of the topochemical aspects of the reduction process in $AFeO_{3-\delta}$ will give us further insight into the oxygen-diffusion pathways of solid oxygen-ion conductors. In addition, currently most materials that conduct oxygen ions are used above 700 °C (refs 13–16), and thus oxygen diffusion below 300 °C is of particular interest in developing low-temperature, oxygen-ion conductor devices. Although oxygen conduction at high temperatures (usually above 700 °C) is a thermally activated hopping process, other mechanisms should be considered for conduction at moderate temperatures, that is below 300 °C to room temperature. Recent oxygen-isotope exchange experiments on $AFeO_{3-\delta}$ revealed the importance of lattice dynamics in terms of structural instability to enhance the oxygen mobility at low temperatures[17]. Oxygen-ion conduction in $La_{1-x}Ba_{1+x}GaO_{4-x/2}$ has been found to proceed by an unusual cooperative process, akin to that of a cog wheel, in Ga_2O_7 units[18]. Atomic reconstruction at the coherent interface in epitaxial ZrO_2:Y_2O_3/$SrTiO_3$ heterostructures increases carrier concentration and decreases activation energy, which gives rise to increased oxygen mobility at room temperature[19]. These results suggest that specific structural features have important roles in oxygen-ion conduction in solids, especially at low temperatures.

It is difficult to examine oxygen migration paths with polycrystalline samples[16], but we expect to see these paths on the atomic scale in single-crystalline materials. As the crystal structures of the oxygen-deficient iron perovskite $AFeO_{3-\delta}$, where $\delta = 1/n$ (n = 1, 2, 4, 8 and ∞) (refs 1,9), become more anisotropic with decreasing n, we should be able to clarify anisotropic oxygen-diffusion behaviours when we examine oriented single-crystalline materials, especially with n = 1 and 2. Using epitaxially grown single-crystalline $CaFeO_{2.5}$ thin films with different orientations, we focused on the reaction mechanism, in terms of the oxygen-diffusion pathways, of the reduction from the brownmillerite $CaFeO_{2.5}$ to the infinite-layer structure $CaFeO_2$.

Results and discussion

The bulk crystal of the brownmillerite $CaFeO_{2.5}$ has a distorted orthorhombic unit cell, a = 5.427 Å, b = 14.763 Å and c = 5.597 Å (space group *Pnma*)[20], which is related to the average perovskite structure with a_p (b_p) ~ d_{101} = 3.896 Å and c_p ~ d_{040} = 3.691 Å. The large anisotropy of a_p/c_p means the orientation of an epitaxially grown $CaFeO_{2.5}$ thin film depends on the substrates[21]. In this study we

[1]Institute for Chemical Research, Kyoto University, Uji, Kyoto 611-0011, Japan, [2]Graduate School of Engineering, Kyoto University, Nishikyo-ku, Kyoto 615-8510, Japan, [3]Université de Rennes 1, Sciences Chimiques de Rennes – UMR 6226, Campus de Beaulieu, Bât 10B, F-35042 Rennes, France.
*e-mail: shimak@scl.kyoto-u.ac.jp

© 2010 Macmillan Publishers Limited. All rights reserved.

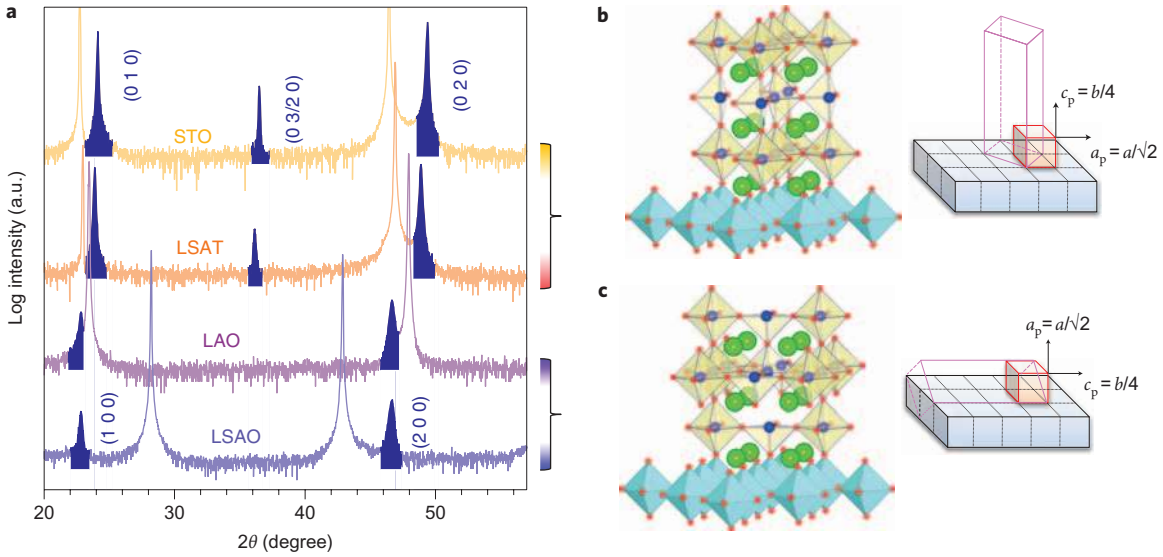

Figure 1 | X-ray diffraction patterns of $CaFeO_{2.5}$ thin films and schematic crystal structures of the films on the substrates. a, X-ray diffraction patterns of as-deposited brownmillerite $CaFeO_{2.5}$ thin films grown on $SrTiO_3$ (STO), $(La_{0.3}Sr_{0.7})(Al_{0.65}Ta_{0.35})O_3$ (LSAT), $LaAlO_3$ (LAO) and $LaSrAlO_4$ (LSAO). The peaks from brownmillerite $CaFeO_{2.5}$ are shown in blue. **b**, Schematic crystal structure of $c_p(b)$-axis-oriented brownmillerite $CaFeO_{2.5}$ grown on a substrate. This orientation structure model represents the growths of the films on the STO and LSAT substrates. **c**, Schematic crystal structure of $CaFeO_{2.5}$ oriented on the a_p-axis. The model represents the growths of the films on the LAO and LSAO substrates.

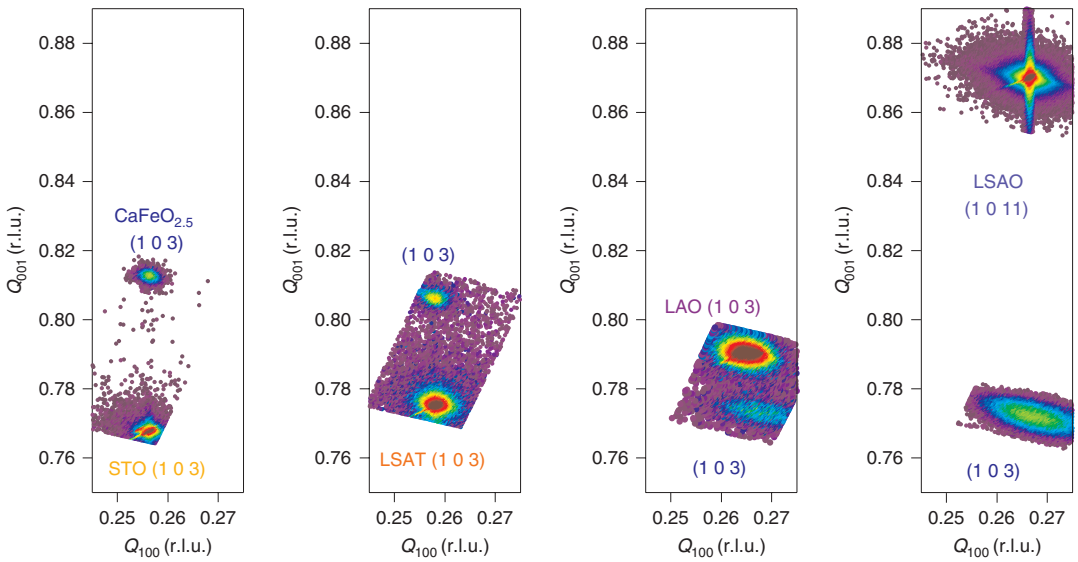

Figure 2 | Logarithmic X-ray diffraction intensity reciprocal lattice space maps of $CaFeO_{2.5}$ thin films. The maps show X-ray diffraction intensities around the (1 0 3) Bragg reflections of brownmillerite $CaFeO_{2.5}$ thin films grown on STO, LSAT, LAO and LSAO. Each film was grown epitaxially on the substrate. The in-plane lattices of $CaFeO_{2.5}$ grown on STO, LSAT and LSAO exactly matched the substrate lattices, but that grown on LAO was slightly different from the LAO substrate lattice. r.l.u. = reciprocal lattice unit.

used four different single-crystalline substrates: $SrTiO_3$ (001) (STO, cubic lattice constant $a = 3.905$ Å), $(La_{0.3}Sr_{0.7})(Al_{0.65}Ta_{0.35})O_3$ (001) (LSAT, $a_p = 3.868$ Å), $LaAlO_3$ (001) (LAO, $a_p = 3.793$ Å) and $LaSrAlO_4$ (001) (LSAO, $a_p = 3.756$ Å). The brownmillerite $CaFeO_{2.5}$ thin film was deposited on each substrate crystal by a pulsed laser-ablation method. As shown in Fig. 1, X-ray diffraction peaks from the brownmillerite $CaFeO_{2.5}$, in addition to those from the substrate lattice, were observed, which confirms that a single-phase $CaFeO_{2.5}$ film was obtained. Interestingly, (0 k 0) and (0 $k/2$ 0) diffraction peaks of $CaFeO_{2.5}$ (indices with respect to the average perovskite unit cell) were found for the films grown on STO and LSAT, whereas only (h 0 0) diffraction peaks were found for the films grown on LAO and LSAO, which have lattices smaller than those of STO and LSAT. The epitaxial growth of the $CaFeO_{2.5}$ thin film on each substrate was confirmed by X-ray diffraction in a reciprocal lattice space around the (1 0 3) Bragg reflection of the average perovskite structure (Fig. 2).

The in-plane and out-of-plane lattice constants of the epitaxially grown $CaFeO_{2.5}$ thin films were obtained from the diffraction peak positions in the reciprocal lattice-space maps and are plotted in Fig. 3. The in-plane lattices of $CaFeO_{2.5}$ grown on STO, LSAT and LSAO exactly matched the substrate lattices, which confirms coherent growth of the films on the substrate crystals. The in-plane lattice constant of $CaFeO_{2.5}$ grown on LAO, however, was slightly different

© 2010 Macmillan Publishers Limited. All rights reserved.

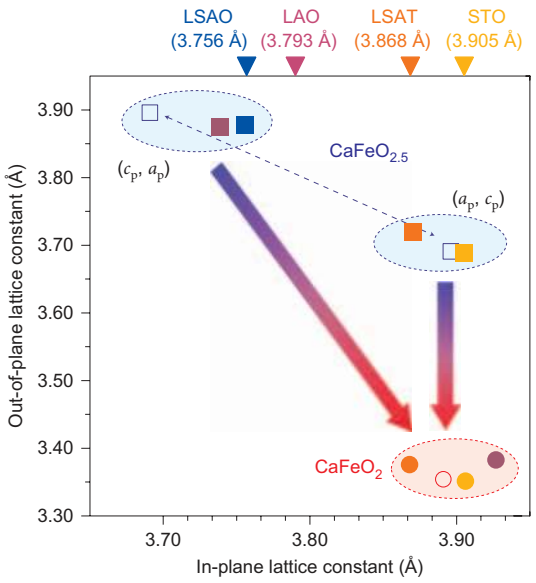

Figure 3 | Lattice constants of brownmillerite $CaFeO_{2.5}$ and infinite-layer structure $CaFeO_2$ thin films. In-plane and out-of-plane lattice constants of as-deposited brownmillerite $CaFeO_{2.5}$ (solid squares) and reduced infinite-layer structure $CaFeO_2$ (solid circles) thin films. Also plotted are the pseudo-tetragonal lattice constants of bulk $CaFeO_{2.5}$, which correspond to a_p (b_p) $\approx d_{101} = 3.896$ Å and $c_p \approx d_{040} = 3.691$ Å (open symbols). The straight dotted line represents isovolume transformation in $CaFeO_{2.5}$. The substrate lattice constants are given at the top of the figure.

from that of LAO, which suggests that the crystal growth of the $CaFeO_{2.5}$ film is relaxed from perfect matching to the substrate lattice. Nevertheless, a single-crystalline $CaFeO_{2.5}$ thin film that kept the epitaxial relationship was obtained on the LAO substrate. The results of X-ray diffraction experiments demonstrated that the deposition on STO and LSAT yielded pseudo-tetragonal $CaFeO_{2.5}$ oriented on the $c_p(b)$-axis, but that on LAO and LSAO yielded $CaFeO_{2.5}$ oriented on the a_p-axis. No other orientation domains were found in any of the films. That the orientation of the brownmillerite $CaFeO_{2.5}$ was affected by the substrate lattice size is reasonable when we compare the lattice mismatches between the films and substrates (Supplementary Table 1). To reduce the lattice energy at the interface, the oriented $CaFeO_{2.5}$ thin film with the smaller lattice mismatch grows easily. Also, each of the $CaFeO_{2.5}$ thin films has almost the same unit-cell volume.

The prepared $CaFeO_{2.5}$ thin films were then reduced by embedding them with CaH_2 powder in evacuated glass tubes and annealing at 240 °C (refs 3,22). A progressive transformation from the (0 k 0) brownmillerite reflections to the (0 0 l) reflections of the infinite-layer structure $CaFeO_2$ was observed during the reduction of the $c_p(b)$-axis-oriented brownmillerite $CaFeO_{2.5}$ thin films grown on the STO and LSAT substrates (Fig. 4). After reduction for 96 hours, no $CaFeO_{2.5}$ diffraction peaks were evident and the film became the infinite-layer structure $CaFeO_2$ oriented on the c-axis. As the positions of the diffraction peaks did not shift during the transformation, we inferred that there were no intermediate oxygen-deficient phases for $CaFeO_{3-\delta}$ with $0.5 < \delta < 1.0$. These changes are quite similar to those seen when the reduction of a $c_p(b)$-axis-oriented $SrFeO_{2.5}$ thin film grown on a $KTaO_3$ substrate produces $SrFeO_2$ oriented on the c-axis with an infinite-layer structure[3]. What is surprising here is that, under the same reduction conditions, the a_p-axis-oriented $CaFeO_{2.5}$ thin film grown on the LAO or LSAO substrate also transformed into $CaFeO_2$ oriented on the c-axis with the infinite-layer structure. This transformation results from the small lattice mismatch of the in-plane lattice of $CaFeO_2$ to the substrate lattices (Supplementary Table 1). Note also that the reduction of the a_p-axis-oriented $CaFeO_{2.5}$ thin films was completed in less than 24 hours (Supplementary Fig. S1), which is much faster than the reduction of the $c_p(b)$-axis-oriented $CaFeO_{2.5}$ thin films on STO and LSAT. X-ray diffraction measurements in a reciprocal lattice space confirmed that the reduction of $CaFeO_{2.5}$ oriented on the a_p-axis did not affect the epitaxial character of the c-axis-oriented $CaFeO_2$ thin film (Supplementary Fig. 2). The in-plane and out-of-plane lattice constants of the infinite-layer $CaFeO_2$ we obtained were, respectively, 3.87–3.93 Å and 3.35–3.38 Å, and the volumes of the reduced films decreased significantly during the reduction process (Fig. 3). We therefore conclude that the c-axis-oriented, single-crystalline $CaFeO_2$ thin films of infinite-layer structure were obtained regardless of the orientation of the precursor $CaFeO_{2.5}$ thin films (Fig. 5).

The result raises important questions as to how the low-temperature oxygen diffusion proceeds in oxides. When we consider the fairly large lateral size of the film sample 60 nm thick (5 mm × 5 mm), it is reasonable to conclude that oxygen atoms are released mainly from the film surface. The oxygen diffusion thus proceeds by chain reaction perpendicular to the film surface using regular vacancy sites in the brownmillerite structure and vacant positions produced by the oxygen release. Two possible reaction processes on the atomic scale can be deduced. In $c_p(b)$-axis-oriented $CaFeO_{2.5}$ thin films on STO and LSAT, oxygen ions should go through the alternate stacking layers of tetrahedra and octahedra in the brownmillerite structure (Fig. 5c). In a_p-axis-oriented $CaFeO_{2.5}$ films on LAO and LSAO, in contrast, oxygen ions diffuse along the a_p or b_p axis, that is the lateral direction of the tetrahedral and octahedral layers (Fig. 5d). The oxygen rearrangement in the a_p-axis-oriented $CaFeO_{2.5}$ films on LAO and LSAO is that which Hayward and Rosseinsky outlined for the change from the perovskite $SrFeO_3$ to the infinite-layer $SrFeO_2$ (ref. 23): one of the oxygen ions in the FeO_4 tetrahedron moves to a vacant site in the octahedron to form the square-planar coordinated FeO_4 in the infinite-layer structure $SrFeO_2$. Our experimental results on the c_p-axis-oriented $CaFeO_{2.5}$ thin film grown on STO or LSAT

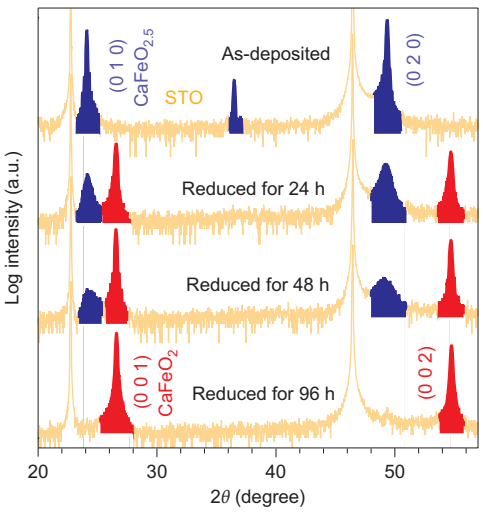

Figure 4 | Progressive change of X-ray diffraction patterns during the reduction of a $CaFeO_{2.5}$ thin film grown on the $SrTiO_3$ substrate. The peaks from brownmillerite $CaFeO_{2.5}$ are shown in blue and those from infinite-layer $CaFeO_2$ in red. A transformation from the brownmillerite $CaFeO_{2.5}$ into the infinite-layer structure $CaFeO_2$ occurred. The film became the c-axis-oriented, infinite-layer structure $CaFeO_2$ after reduction for 96 hours. The positions of the diffraction peaks do not shift during the transformation, so no intermediate oxygen-deficient phases for $CaFeO_{3-\delta}$ with $0.5 < \delta < 1.0$ exist.

© 2010 Macmillan Publishers Limited. All rights reserved.

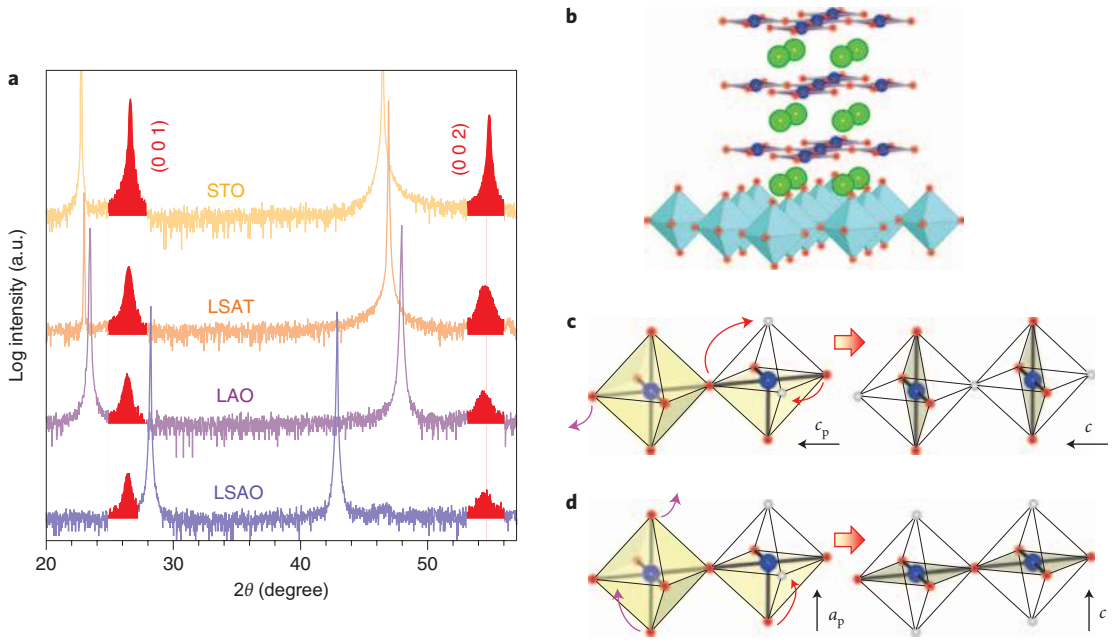

Figure 5 | X-ray diffraction patterns of $CaFeO_2$ thin films and schematic crystal structure of the films on the substrates. a, X-ray diffraction patterns of reduced infinite-layer structure $CaFeO_2$ thin films on STO, LSAT, LAO and LSAO. The peaks from infinite-layer $CaFeO_2$ are shown in red. The data for films on STO and LSAT were obtained after reduction for 96 hours and those for films on LAO and LSAO were obtained after reduction for 24 hours. **b**, Schematic crystal structure of the *c*-axis-oriented, infinite-layer structure $CaFeO_2$ on each substrate of STO, LSAT, LAO or LSAO. **c**, Schematic model of the oxygen-diffusion pathway and the rearrangement from tetrahedral to square-planar coordination in FeO_4. This model represents the change in films on the STO and LSAT substrates. **d**, Same as (**c**), but for the change in films on the LAO and LSAO substrates. The oxygen diffusion in the brownmillerite structure is highly anisotropic; significantly higher in the a_pb_p plane (**d**) than along the c_p-axis (**c**).

clearly demonstrate that the oxygen rearrangement at 240 °C also proceeds by a different route, one in which two oxygen ions in the FeO_4 tetrahedron are involved to form the square-planar, coordinated FeO_4 in $CaFeO_2$ with the infinite-layer structure.

An important difference between the two diffusion pathways concerns kinetic aspects of release and rearrangement processes in the brownmillerite-structure framework. The complete reduction of the $c_p(b)$-axis-oriented $CaFeO_{2.5}$ thin film takes about four times longer than that of the the film oriented on the a_p-axis, so the activation energy for the release and rearrangement of oxygen ions along the $c_p(b)$-axis is much higher than that for the release and rearrangement of oxygen ions along the a_p-axis. This implies that oxygen diffusion in the brownmillerite structure is highly anisotropic; significantly higher in the a_pb_p plane than along the stacking direction of the tetrahedral and octahedral layers.

Methods

The brownmillerite $CaFeO_{2.5}$ precursor ceramic target was prepared in a solid-state reaction of $CaCO_3$ and Fe_2O_3. A mixture of the raw materials was fired at 1200 °C in air for 36 hours with intermediate grinding. The $CaFeO_{2.5}$ precursor thin films were deposited on substrates by pulsed laser deposition using a KrF excimer laser pulse ($\lambda = 248$ nm) (COHERENT COMPex-Pro 205 F). The oxygen partial pressure during the depositions was 10^{-5} torr, and the substrate temperature was monitored with a pyrometer and kept at 675 °C. Single-crystal substrates of $SrTiO_3$ (001), $(La_{0.3}Sr_{0.7})(Al_{0.65}Ta_{0.35})O_3$ (001), $LaAlO_3$ (001) and $LaSrAlO_4$ (001) were used in this study. Thicknesses of the deposited films were estimated by Raue fringe in X-ray diffraction measurements as ~60 nm. The deposited $CaFeO_{2.5}$ thin-film samples were embedded with about 0.25 g of CaH_2 powder in glass tubes in an argon-filled glove box and the tubes were sealed under vacuum conditions, after which they were kept at 240 °C for 8–96 hours. The residual products and unreacted CaH_2 on the film surface were removed by rinsing in 2-butanone. Crystal structures of the films were examined by $2\theta-\omega$ scans and reciprocal space mappings of X-ray diffraction with Cu-K_α radiation. A four-circle diffractometer (PANalytical X'Pert MRD) was used for the measurement, and diffraction intensities in a reciprocal space (Q_{100}, Q_{001}) area were measured.

Received 26 June 2009; accepted 4 January 2010; published online 7 February 2010

References

1. Tsujimoto, Y. *et al.* Infinite-layer iron oxide with a square-planar coordination. *Nature* **450,** 1062–1065 (2007).
2. Tassel, C. *et al.* Stability of the infinite layer structure with iron square planar coordination. *J. Am. Chem. Soc.* **130,** 3764–3765 (2008).
3. Inoue, S. *et al.* Single-crystal epitaxial thin films of $SrFeO_2$ with FeO_2 'infinite layers'. *Appl. Phys. Lett.* **92,** 161911 (2008).
4. Tassel, C. *et al.* $CaFeO_2$: a new type of layered structure with iron in a distorted square planar coordination. *J. Am. Chem. Soc.* **131,** 221–229 (2009).
5. Hayward, M. A. & Rosseinsky, M. J. Anion vacancy distribution and magnetism in the new reduced layered Co(II)/Co(I) phase $LaSrCoO_{3.5-x}$. *Chem. Mater.* **12,** 2182–2195 (2000).
6. Hayward, M. A. *et al.* The hydride anion in an extended transition metal oxide array: $LaSrCoO_3H_{0.7}$. *Science* **295,** 1882–1884 (2002).
7. Blundred, G. D., Bridges, A. B. & Rosseinsky, M. J. New oxidation states and defect chemistry in the pyrochlore structure. *Angew. Chem. Int. Edn* **43,** 3562–3565 (2004).
8. Takeda, Y. *et al.* Phase relation in the oxygen nonstoichiometric system $SrFeO_x$ ($2.5 < x < 3$). *J. Solid State Chem.* **63,** 237–249 (1986).
9. Hodges, J. P. *et al.* Evolution of oxygen-vacancy ordered crystal structures in the perovskite series $Sr_nFe_nO_{3n-1}$ ($n = 2$, 4, 8, and ∞), and the relationship to electronic and magnetic properties. *J. Solid State Chem.* **151,** 190–209 (2000).
10. Grenier, J.-C. *et al.* Electrochemical oxygen intercalation into oxide networks. *J. Solid State Chem.* **96,** 20–30 (1992).
11. Hayashi, N., Terashima, T. & Takano, M. Oxygen-holes creating different electronic phases in Fe^{4+}-oxides: successful growth of single crystalline films of $SrFeO_3$ and related perovskites at low oxygen pressure. *J. Mater. Chem.* **11,** 2235–2237 (2001).
12. Fisher, C. A. J. & Islam, M. S. Mixed ionic/electronic conductors $Sr_2Fe_2O_5$ and $Sr_4Fe_6O_{13}$: atomic-scale studies of defects and ion migration. *J. Mater. Chem.* **15,** 3200–3207 (2005).
13. Goodenough, J. B. Oxide-ion electrolytes. *Annu. Rev. Mater. Res.* **33,** 91–128 (2003).
14. Steele, B. C. H. & Heinze, A. Materials for fuel-cell technologies. *Nature* **414,** 345–352 (2001).
15. Ormerod, R. M. Solid oxide fuel cells. *Chem. Soc. Rev.* **32,** 17–28 (2003).
16. Atkinson, A. *et al.* Advanced anodes for high-temperature fuel cells. *Nature Mater.* **3,** 17–27 (2004).
17. Paulus, W. *et al.* Lattice dynamics to trigger low temperature oxygen mobility in solid oxide ion conductors. *J. Am. Chem. Soc.* **130,** 16080–16085 (2008).

© 2010 Macmillan Publishers Limited. All rights reserved.

18. Kendrick, E., Kendrick, J., Knight, K. S., Iskam, M. S. & Slater, P. R. Cooperative mechanisms on fast-ion conduction in gallium-based oxides with tetrahedral moieties. *Nature Mater.* **6,** 871–875 (2007).
19. Garcia-Barriocanal, J. *et al.* Colossal ionic conductivity at interfaces of epitaxial ZrO_2:Y_2O_3/$SrTiO_3$ heterostructures. *Science* **321,** 676–680 (2008).
20. Redhammer, G. J., Tippelt, G., Roth, G. & Amthauer, G. Structural variations in the brownmillerite series $Ca_2(Fe_{2-x}Al_x)O_5$: single-crystal X-ray diffraction at 25 °C and high-temperature X-ray powder diffraction (25 °C ≤ T ≤ 1000 °C). *Am. Mineral.* **89,** 405–420 (2004).
21. Rossell, M. D. *et al.* Structure of epitaxial $Ca_2Fe_2O_5$ films deposited on different perovskite-type substrates. *J. Appl. Phys.* **95,** 5145–5152 (2004).
22. Kawai, M. *et al.* Reversible changes of epitaxial thin films from perovskite $LaNiO_3$ to infinite-layer-structure $LaNiO_2$. *Appl. Phys. Lett.*, **94,** 082102 (2009).
23. Hayward, M. A. & Rosseinsky, M. J. Cool conditions for mobile ions. *Nature* **450,** 960–961 (2007).

Acknowledgements

We thank K. Yoshimura for his support during this work, and K. Matsumoto and A. Sakaiguchi for discussions. This work was supported in part by Grants-in-Aid for Scientific Research (19GS0207 and 19052004), by the Global Centers of Excellence Program 'International Center for Integrated Research and Advanced Education in Materials Science' and by a grant for the Joint Project of Chemical Synthesis Core Research Institutions from the Ministry of Education, Culture, Sports, Science and Technology of Japan. The work was also partly supported by a European Master programme, Master in Materials Science Exploiting European Large Scale Facilities.

Author contributions

S.I. and Y.S. conceived and designed the study. S.I. and M.K. performed the experiments with the help of N.I. H.K. and W.P. contributed the main discussion on oxygen diffusion in iron oxides. All of the authors discussed the results. S.I. and Y.S. wrote the manuscript with comments from H.K. and W.P.

Additional information

The authors declare no competing financial interests. Supplementary information accompanies this paper at www.nature.com/naturechemistry. Reprints and permission information is available online at http://npg.nature.com/reprintsandpermissions/. Correspondence and requests for materials should be addressed to Y.S.

© 2010 Macmillan Publishers Limited. All rights reserved.